# Axial Hydrogen at C7 Position and Bumpy Tetracyclic Core Markedly Reduce Sterol's Affinity to Amphotericin B in Membrane

Yasuo Nakagawa, Yuichi Umegawa, Kenichi Nonomura, Naohiro Matsushita, Tetsuro Takano, Hiroshi Tsuchikawa, Shinya Hanashima, Tohru Oishi, Nobuaki Matsumori,* and Michio Murata*

Department of Chemistry, Graduate School of Science, Osaka University, 1-1 Machikaneyama, Toyonaka, Osaka 560-0043, Japan

S Supporting Information

ABSTRACT: The interaction of amphotericin B (AmB) with fungal ergosterol (Erg) is stronger than its interaction with mammalian cholesterol (Cho), and this property of AmB as an antifungal drug is thought to be responsible for its selective toxicity toward fungi. However, the mechanism by which AmB recognizes the structural differences between sterols, particularly minor difference in the sterol alicyclic portion, is largely unknown. Thus, to investigate the mode of interaction between AmB and the sterol core, we assessed the affinity of AmB to various sterols with different alicyclic structures. Ion flux assays and UV spectral measurements clearly revealed the importance of the Δ7-double bond of the sterol B-ring for interaction with the drug. AmB showed lower affinity for triene sterols, which have double bonds at the Δ5, Δ7, and Δ9 positions. Intermolecular distance measurements by $^{13}C\{^{19}F\}$ rotational echo double resonance (REDOR) revealed that the AmB macrolide ring is in closer contact with the steroid core of Erg than it is with the Cho core in the membrane. Conformational analysis suggested that an axial hydrogen atom at C7 of Δ5-sterol (**2**, **6**) and the protruded A-ring of Δ5,7,9-sterol (**4**, **8**) sterically hampered face-to-face contact between the van der Waals surface of the sterol core and the macrolide of AmB. These results further suggest that the α-face of sterol alicycle interacts with the flat macrolide structure of AmB.
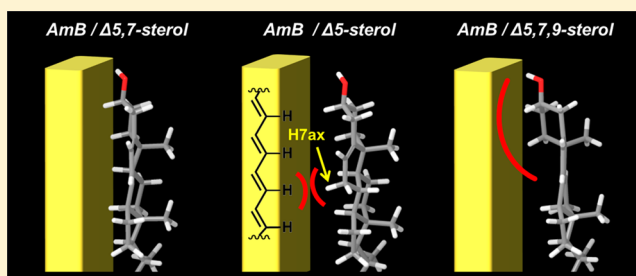
Sterols in cell membranes are major targets of bioactive natural products such as polyene macrolides,[1,2] polyene polyols,[3-6] and peptides,[7,8] some of which are clinically used as antibiotics due to their unique biological and pharmacological activities through their direct interactions with sterols.[3,8,9] Therefore, knowledge of the mechanisms underlying intermolecular recognition between bioactive compounds and membrane sterols is particularly important, because such binding underlies the molecular basis of their selective toxicity. A thorough understanding of the biological effects of these natural compounds may lead to the development of more efficacious drugs with less toxicity.

Amphotericin B (AmB) is a polyene macrolide antibiotic that is widely used to treat deep-seated fungal infections and shows sterol-derived selective toxicity.[10,11] Despite the severe side effects of AmB, the occurrence of fungal strains resistant to other drugs makes it irreplaceable.[12,13] Although many possible molecular mechanisms of AmB such as surface adsorption model[14,15] and oxidation damage[16,17] have been discussed, it is widely accepted that the mode of action of the drug is attributable to the formation of ion-permeable channels across cell membranes with sterols, which disrupt the physiological ion balance of fungal cells.[1,14,18] Several AmB molecules self-assemble to produce ion channels selectively in fungal cell membranes mainly because their interaction with fungal ergosterol (Erg) stabilizes the channel complex more efficiently

than does the interaction with mammalian cholesterol (Cho).[1,9,19] Recent studies by Burke's group have suggested that sequestering Erg from the cell membrane is the primary mode of antifungal action of AmB, while channel formation is a secondary mechanism.[20,21] Either way, the selective toxicity of AmB for fungi can be explained by its higher affinity for Erg than for Cho in phospholipid membranes.[22,23] For this reason, the effects of sterols and other lipids on formation of the AmB-induced molecular assemblage have been investigated by various techniques, including UV/CD spectroscopy,[23-26] ion-flux assays,[23,27-29] solid state NMR,[9,20,30-32] and molecular simulations.[33-37] However, it is unclear which sterol substructure is most critical for the interactions with AmB. Using ion-flux assays and SPR techniques,[38] we recently investigated the structure—activity relationship for sterol by testing a series of Erg analogues with different side-chains. We found that the C24 methyl group and the Δ22 double bond in Erg significantly enhanced its affinity to AmB equally and independently, and such strong interactions between Erg side-chains and AmB were also confirmed by solid-state NMR as we reported previously.[31]
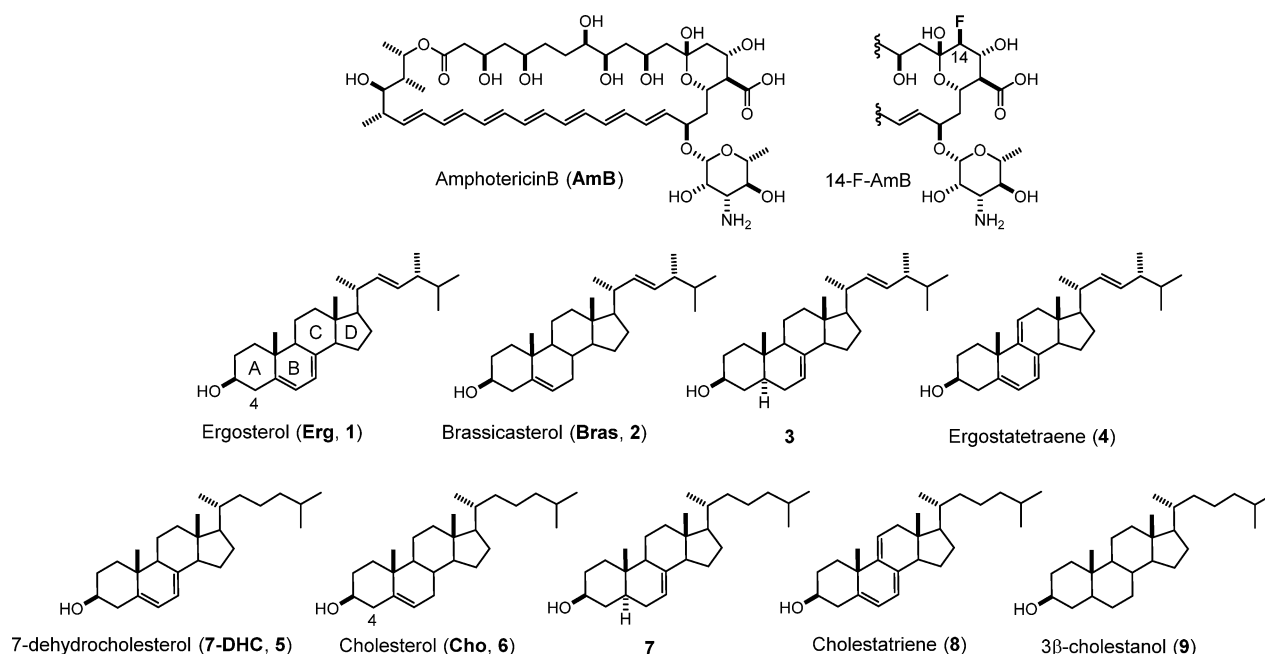
Figure 1. Chemical structures of amphotericin B and sterols used in this study. The sterols in the upper and lower rows have the side chain structures of Erg and Cho, respectively.

Regarding the tetracyclic sterol core, it is generally accepted that the presence of a conjugated double bond on the B-ring is very important for interaction with AmB. By observing the change in the UV–vis absorption intensity of the drug, Bittman's group demonstrated that Erg and 7-dehydrocholesterol (7-DHC) interact with AmB with higher affinity than they do with Cho, and suggested that the double bond on the B-ring, particularly the Δ7 double bond, is one of the sites responsible for high affinity to AmB.[25] One possible explanation for the effect of the double bonds on the steroid core is that they decrease its flexibility, which stabilizes the van der Waals (VDW) interaction with the rigid macrolide of AmB,[24,33,37] while another explanation is that the negative electrostatic potential on the steroid core of Erg caused by the additional double bond on the B-ring enhances electrostatic interaction with the heptaene moiety of AmB.[39,40] However, the detailed recognition mechanism of AmB and the sterol core is still unclear, although it has been the subject of numerous studies. Atomistic studies have been hampered by a lack of systematic and quantitative experimental data, because AmB–sterol analysis is mainly based on molecular simulations and/or fragmental information mostly derived from commercially available sterol analogues.

To investigate how structural alternation in double bond systems in the sterol core affects AmB–sterol interaction, we systematically and quantitatively evaluated the affinity of sterols having various double bond systems on the basis of K^+-flux activity and the UV spectra of AmB. Regarding the two most important sterols, Erg and Cho, we performed solid state NMR experiments to obtain direct evidence of the intermolecular contact between the sterol core and the macrolide of AmB. Figure 1 depicts the sterols used in this study: sterols with Δ5,7-conjugated double bonds, Δ5 or Δ7 double bonds, Δ5,7,9 conjugated trienes, or no double bonds in the alicyclic structure. For comparison, we simultaneously compared two types of side chain structures: Erg-type compounds **1**, **2**, **3**, and **4**, and Cho-type compounds **5**, **6**, **7**, **8**, and **9**.

■ MATERIALS AND METHODS

Materials. Sterol analogues 5-dihydro-ergosterol **3**[41] and ergostatetraene **4**[42] were synthesized from Erg, and 5-dihydro-7-dehydrocholesterol **7**[41] and cholestatriene **8**[43] were synthesized from 7-dehydrocholesterol (7-DHC), as described in previous reports. 4-^{13}C-ergosterol was synthesized from Erg in a manner similar to that used by Pelc's group for the synthesis of 4-^{14}C-ergosterol (synthesis details are described in the Supporting Information).[44] 4-^{13}C-cholesterol was purchased from Cambridge Isotope Laboratories (Tewksbury, MA, USA). AmB, Cho, carbonyl cyanide-p-trifluoromethoxyphenylhydrazone (FCCP), 2′,7′-bis(carboxyethyl)-4(5)-carboxyfluorescein (BCECF), and valinomycin were purchased from Nacalai Tesque (Kyoto, Japan). Erg and 3-β-cholestanol were obtained from Tokyo Kasei (Tokyo, Japan), Bras was obtained from Tama Biochemical Co. Ltd. (Tokyo, Japan), 7-DHC was obtained from MP Biomedicals Inc. (Santa Ana, CA, USA), and 1-palmitoyl-2-oleoyl-sn-glycero-3-phosphocholine (POPC) was obtained from NOF Corp. (Tokyo, Japan). All other chemicals were obtained from standard vendors and were of analytical grade. It is known that the AmB is sensitive to atmospheric oxygen and the light. Therefore, AmB was treated under Ar atmosphere and low light condition.

K^+ Flux Assays Using BCECF. The experiments were performed as described in our previous reports.[19,38] We chose POPC as membrane phospholipid since our previous study revealed that POPC-based bilayers were a better medium for examining the sterol effects on AmB's membrane-permeabilizing activity.[9] In addition, we previously adopted POPC to investigate the effects of side-chain structures of sterols on AmB–sterol interactions.[38] POPC (14.8 μmol) and a corresponding sterol analogue (Erg (**1**), Bras (**2**), 5-dihydroergosterol (**3**), ergostatetraene (**4**), 7-DHC (**5**), Cho (**6**), 5-dihydro-7-dehydrocholesterol (**7**), cholestatriene (**8**), or cholestanol (**9**); 0.78 μmol) were dissolved in CHCl$_3$ and evaporated to produce a thin film. After the film was dried in vacuo overnight, it was suspended in phosphate buffer (0.15 M

potassium phosphate and 76 μM BCECF, pH 5.8) by sonication and vortexing, and frozen and thawed 5 times to produce large vesicles. The resulting suspension was sized by extrusion (19 times) through a polycarbonate filter (200 nm pore size) using a Liposofast syringe extruder (Avestin Inc., Ottawa, Canada) to form large unilamellar vesicles entrapping BCECF (LUVs). The BCECF remaining outside the liposome was removed by gel filtration using Sepharose 4B (Sigma-Aldrich, St. Louis, MO, USA) and 0.15 M potassium phosphate buffer (pH 5.8). After determining the lipid concentration of the suspension by a Phospholipid C-test (Wako Pure Chemical Industries, Ltd., Tokyo, Japan), it was diluted with 0.15 M potassium phosphate buffer (pH 5.8) to 0.5 mM. To 5 mL liposome solution was added 1 mM FCCP in EtOH (50 μL), and the resulting suspension was cooled to 6 °C. In this study, AmB was added to the liposome suspension at two different times to allow study of the early stage of channel formation and steady state channel formation.[38] For the early stage experiment, the liposome solution was poured into a cuvette containing 1.8 mL of K_2HPO_4 (0.15 M, pH 9.2) positioned in a fluorescent spectrometer (FP-6600, JASCO, Tokyo, Japan) equipped with a magnetic stirrer, and 10 μL of 32 μM AmB in DMSO was added to the stirred solution (final concentration of AmB was 0.16 μM). The time-dependent change in the liposomal pH that was caused by K^+ influx was monitored by the increase in the fluorescence intensity (excitation, 500 nm; emission, 535 nm) at 6 °C. After fluorescent recording for 70 s, potassium ionophore valinomycin in MeOH (5 mM, 10 μL) was added to obtain the fluorescence intensity corresponding to 100% exchange (F_{max}). The resulting time-dependent fluorescence intensity change was normalized to the F_{max} value. For steady state experiments, AmB in DMSO (32 μM, 10 μL) was added to the liposome solution (0.5 mM, 200 μL) and incubated for 3 h at 6 °C to allow for equilibration of the AmB channel forming process. The resulting suspension was poured into a cuvette containing 1.8 mL of K_2HPO_4 (0.15 M, pH 9.2) positioned in a fluorescent spectrometer equipped with a magnetic stirrer, and the fluorescence change was recorded and expressed as a percentage of F_{max} as described above. For quantitative analysis, the initial K^+/H^+ exchange rate r was calculated from the fluorescence intensity change immediately after the addition of AmB by curve fitting to the exponential curve ($F = A(1 - \exp(-t/T))$). The r value (presented as A/T ($t = 0$)) was expressed as the rate of K^+ entering into the liposomes per second with respect to the initial $[K^+]$ difference between the outside and inside of the liposomes. The experiments were performed in triplicate and the averages of the r values and standard errors were obtained.

UV Spectral Measurements. AmB (95 nmol) and POPC (3.0 μmol) were dissolved in CH_2Cl_2/MeOH (2:1) (20% of POPC was replaced with sterols for the measurements of liposomes containing sterols). The samples were evaporated and dried in vacuo overnight to produce a thin film. The resulting lipid film was suspended in 8% sucrose aqueous solution (2 mL) by vortexing and sonication, and the lipid suspension was frozen and thawed 5 times to produce large vesicles. Next, 300 μL of the resulting suspension was diluted with 8% sucrose aqueous solution (2400 μL) and used for the spectral measurements. UV spectra were recorded with a V-630BIO spectrophotometer (Shimadzu, Kyoto, Japan) with a 1.0 cm path length quartz cell at 23 °C at 0.1 nm intervals over a wavelength range of 300–450 nm.

Solid-State NMR Measurements. POPC (39.6 μmol) and 4-^{13}C-sterol (4.4 μmol) were added with AmB or 14-F-AmB (4.4 μmol), and completely dissolved in MeOH/CHCl$_3$. Then the organic solvent was evaporated and dried in vacuo overnight to yield thin film. The obtained film was hydrated with 35 μL of 10 mM HEPES buffer (pH 7.0) and 1 mL H_2O, and suspended by vortexing and sonication. The suspension was subjected to five freeze–thaw cycles (liquid nitrogen and water bath), and then lyophilized overnight. After rehydration with D_2O (50 wt %), the sample was immediately packed into a glass tube. The tube was inserted into a φ 5 mm MAS rotor. The CP-MAS ^{13}C NMR and ^{13}C{^{19}F}REDOR spectra were recorded on a Chemagnetics CMX300 (Agilent Technologies, Santa Clara, CA, USA) spectrometer at a 75 MHz ^{13}C resonance frequency with a MAS frequency of 5000 ± 2 Hz. The temperature of the air was maintained at 30 ± 1 °C or −30 ± 2 °C. The spectral width was 30 kHz. Typically, the π/2 pulse width for ^{1}H was 3.1 μs and the π pulse widths for ^{13}C and ^{19}F were 6.6 and 8.5 μs, respectively. The contact time for cross-polarization transfer was set to 1.0 ms. The spectra were acquired with a recycle delay of 2 s under TPPM ^{1}H-decoupling[45] with a field strength of 81 kHz, and xy-8 phase cycling[46] was used for ^{19}F π pulses in the ^{13}C{^{19}F}REDOR.

Conformational Analysis of Sterol Analogues by MO Calculation. All calculations were carried out with Macromodel software version 9.9 (Schrödinger, New York, NY, USA) installed on a personal computer running the Windows 7 operating system. The initial structures for DFT calculations were built using a molecular mechanics-based conformational search followed by energy minimization. The sampling of the conformational space was performed with a mixed torsional/low-mode sampling (MCMM/LMCS) method.[47] The OPLS 2005 force field[48] implemented in the Macromodel program was used for the conformational searches with 5000 steps. Energy minimization was carried out using the Polak-Ribiele conjugate gradient (PRCG)[49] method with 7000 maximum iterations, and torsion angles of the entire molecule were optimized in vacuum. The resulting conformers were minimized and redundant conformers were eliminated. Energy minimization was carried out using the truncated Newton conjugate gradient (TNCG) method[50] with 7000 maximum iterations. The lowest energy conformer was subjected to further gas-phase geometry optimization in Jaguar software version 7.9 (Schrödinger, New York, NY, USA) using the density functional theory (DFT)[51] with the B3LYP/6–31G(d,p)[52] functional and basis set combination.

■ RESULTS AND DISCUSSION

K^+/H^+ Exchange Assays. In order to examine the effect of sterol alicyclic structures on the ion-channel activity of AmB, K^+-influx assays were carried out using POPC liposomes that contained sterol analogues **1–9**. In this study, two types of K^+ flux measurements were carried out based on methods available in a previous report from our group; one method focused on the very early stage of AmB–sterol complex formation and the other focused on steady state AmB–sterol complex formation.[38] It is thought that the early stage experiments measured binding of AmB to the membrane and the formation rate of ion channel complexes, while the steady state experiments predominantly evaluated the stability of the channels. Therefore, the results of these experiments potentially contain the specific information regarding the effects of sterol types at each step of the AmB channel formation process.
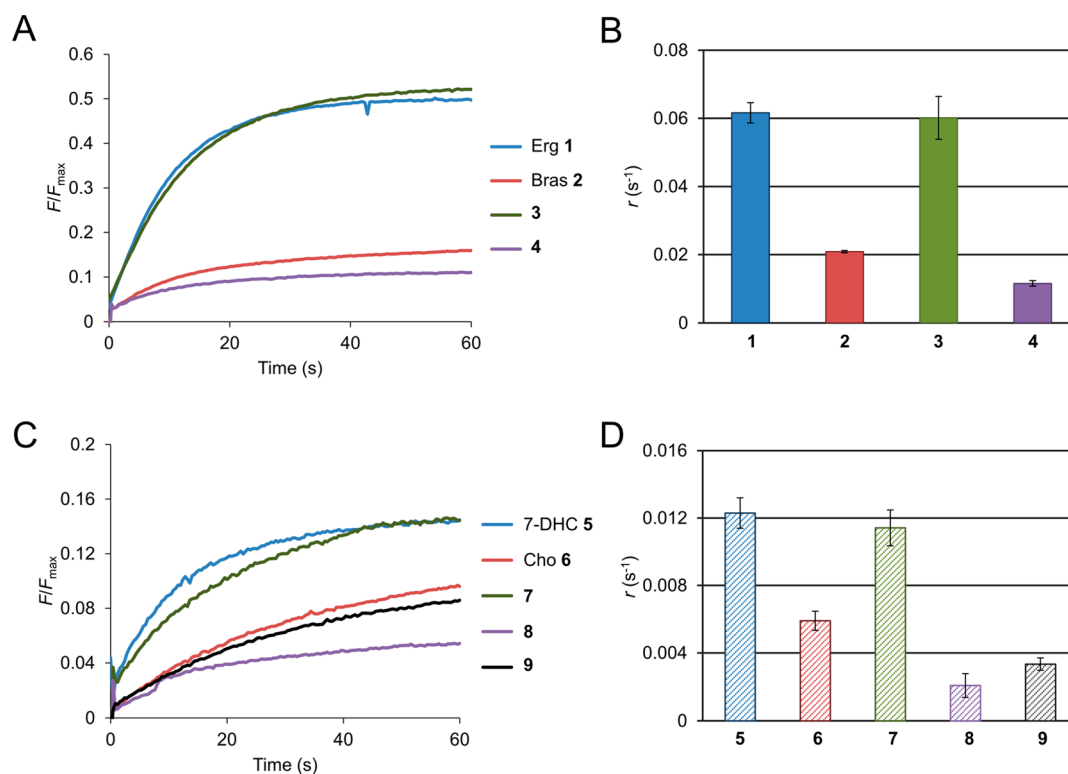
Figure 2. Sterol effects on the early stage of AmB-induced K^+-influx. (A,C) Fluorescence intensity (F/F_{max}) change was monitored by the pH-sensitive dye BCECF. (B,D) K^+/H^+ exchange rate r for sterol analogue-containing liposomes. The liposomes were prepared from POPC with admixed 5 mol % sterol analogues. The figures show the results at $R_{(AmB/lipid)} = 3.16 \times 10^{-3}$. In a sterol-free POPC membrane, AmB slightly increased ion permeability ($r = 0.00095 \pm 0.00029$).
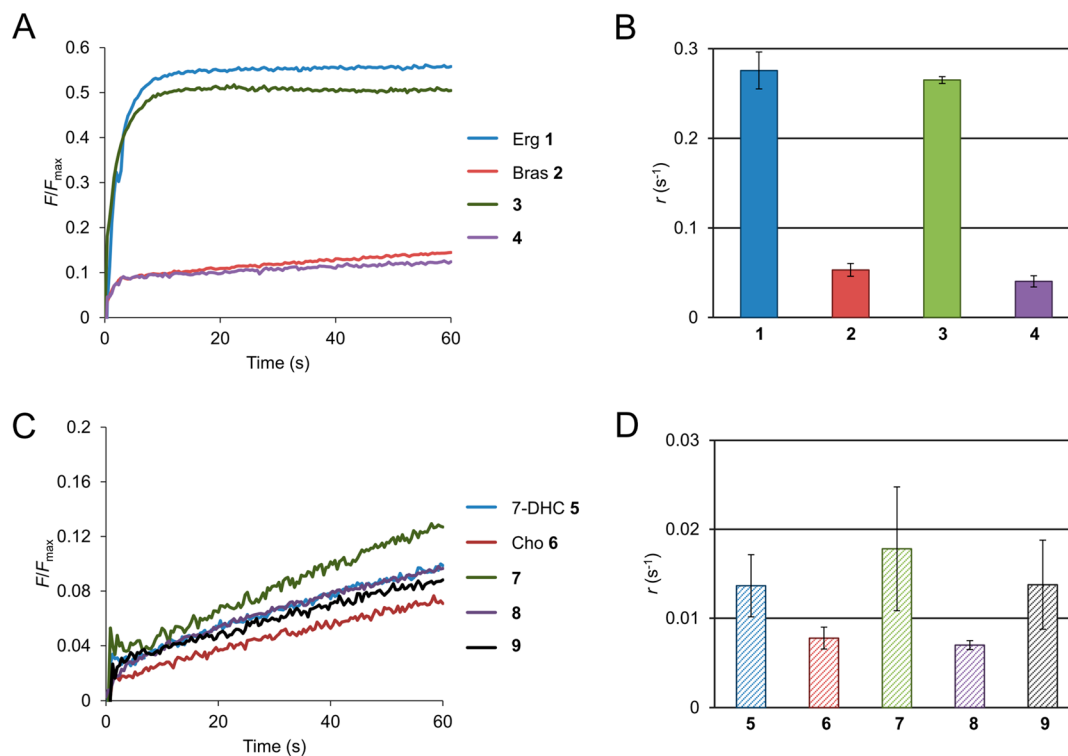

Figure 3. Sterol effects on steady state AmB-induced K^+-influx. (A,C) Fluorescence intensity (F/F_{max}) change was monitored with the pH-sensitive dye BCECF. (B,D) K^+/H^+ exchange rate r for sterol analogue-containing liposomes. The liposomes were prepared from POPC with admixed 5 mol % sterol analogues. The figure shows the results at $R_{(AmB/lipid)} = 3.16 \times 10^{-3}$. In a sterol-free POPC membrane, AmB slightly increased ion permeability ($r = 0.0023 \pm 0.00081$).
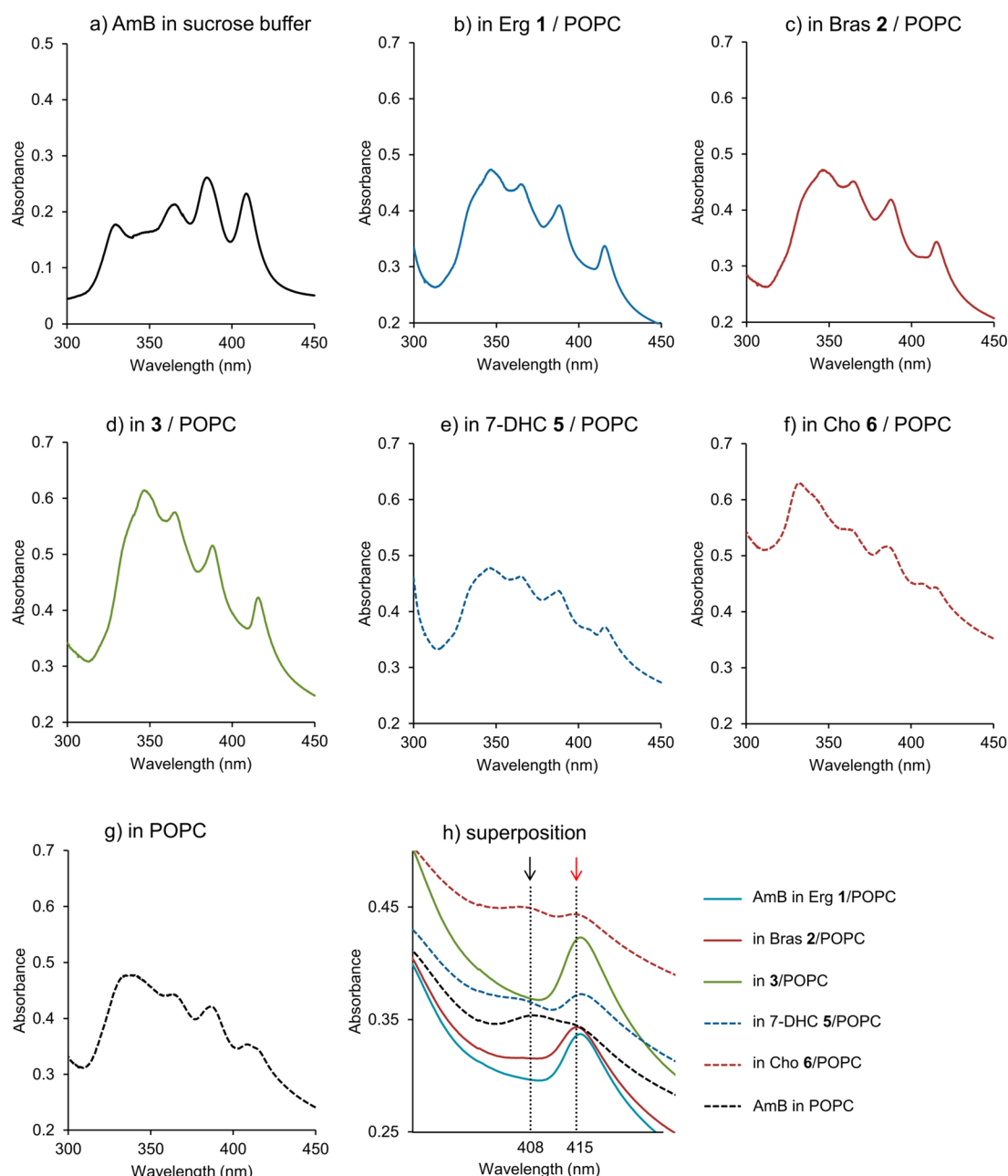
Figure 4. UV spectra of AmB in sucrose buffer (a) and sterol-containing POPC membranes (b−g) at $R_{(AmB/lipid)} = 3.16 \times 10^{-2}$. (h) Superposition of the spectra around 390−430 nm. The red and black arrows indicate components residing in the membrane (415 nm) and water (408 nm) phases, respectively. The molar ratio of POPC:sterol was 4:1, and the concentration of AmB was 5.27 μM in sucrose buffer. A rise of the baseline is due to the scattering of light from the liposome. The UV spectrum of the pure POPC liposome was shown in Supporting Information Figure S3.

In the early stage experiments, a clear dependence on alicyclic structure was observed (Figure 2A,C), and the K$^+$/H$^+$ exchange rate r was calculated from the initial change in fluorescence intensity (Figure 2B,D). For the Erg side-chain series (Figure 2B), it was found that **2**, which had the only Δ5-double bond on the core, produced significantly less effect on AmB-induced K$^+$ flux than **1**. Interestingly, **3**, which has one double bond at a different position from that of **2**, showed comparable activity to **1**. Further addition of one double bond at the Δ9 position (**4**) of **1** markedly reduced the permeabilizing activity of AmB, although the addition of another double bond on the steroid ring was expected to enhance the π−π electronic interaction and/or the VDW interaction with AmB. The sterols that shared a side chain

structure with Cho **6** showed a similar tendency to that observed in the Erg side-chain series, but were markedly less efficacious (Figure 2C,D).[38] Sterols **5** and **7** effectively promoted K$^+$/H$^+$ exchange, while the other Cho derivatives reduced the K$^+$-influx of AmB. These results clearly demonstrated that the K$^+$-influx activity of AmB does not depend on the number of double bonds, but on their position in the tetracyclic core. Considering a similar dependence of the AmB activity between the core structures with the Erg side chain and those with the Cho side chain, the results strongly suggested that side chain and alicyclic structures contributed to the flux-promoting activity in a largely independent manner.

Figure 3 shows the fluorescence measurements of sterol-containing liposomes in the steady state of channel formation

after incubation with AmB for 3 h (A,C) and the rates of K^+/H^+ exchange (B,D), which showed roughly similar tendencies to those observed in the early stage experiments in Figure 2, although the flux-promoting activity of **1** and **3** were somewhat enhanced. In the steady state experiments, the flux-promoting activities were largely dependent on the stability of the AmB−sterol complex. These results indicate that, as is the case with the side chain structure, the alicyclic structure of the sterol influences the stability of the AmB−sterol complex.[38] We also evaluated the lifetime of the AmB−sterol complex using SPR experiments (see Supporting Information), and confirmed that the lifetime of the channel strongly depends on the alicyclic structure of its sterol component, and the influence of the structure was found to be roughly similar to that observed in the steady state K^+-influx assays within each series of sterols bearing an Erg-type side chain or Cho-type one.

UV Spectra of AmB in Sterol-Containing Membranes. To further examine the influence of the unsaturation profile of the sterol core on formation of the AmB−sterol complex, we recorded the UV spectra of AmB in sterol-containing liposomes (Figure 4). It is generally accepted that the absorption maxima λ_{max} at 408, 385, and 365 nm of AmB in aqueous buffer are chiefly due to the monomeric form of the drug, while the absorption band at 328 nm is indicative of the aggregated form (Figure 4).[53] In the Erg-containing POPC membrane, the longest wavelength peak shifted to 415 nm (Figure 4, inset), which was thought to be caused by increased hydrophobicity around the heptaene moiety of AmB,[53] indicating that the drug bound efficiently to the POPC bilayers. In contrast, some of other sterol-containing and sterol-free membranes gave rise to the absorption bands that consisted of two components with λ_{max} at 415 and 408 nm; these two peaks implied the coexistence of AmB in the membrane and in the water phase, where the intensity ratio of the peaks can be related to the stability of the AmB−sterol complex. Interestingly, the ratio changes by the sterol core structures and increases in the order of sterol-free < Cho **6** < 7-DHC **5** < Bras **2**. This tendency of the complex formation correlates well with the potency of sterol in the K^+-flux assays. The influence of the core structure on the AmB−sterol complex formation is also observed by the shorter wavelength shift for the peak around 320−350 nm. This hypsochromic shift is thought to strongly depend on the distance between neighboring heptaene chromophores in parallel AmB-AmB orientation; a shorter distance causes a larger hypsochromic shift.[30,54] The absorption patterns of the sterol-containing membranes around 320−350 nm were quite variable, which probably reflects the different molecular assemblages formed in each sterol-containing membrane. We have previously reported that AmB forms dense aggregates in Cho-containing or sterol-free membrane, and the aggregates were largely phase-separated from the lipid bilayer and did not induce membrane permeabilization.[9,30] Thus, the hypsochromic absorption around 330 nm observed for sterol-free and Cho-containing membranes is thought to be due to these dense aggregates. Conversely, the sterols that induced stronger ion flux-promoting activities gave rise to the absorption peak at around 350 nm. These changes indicate that the distance between neighboring heptaene moieties is increased by the formation of similar channel assemblages as we suggested by solid state NMR.[30] Therefore, the absorption bands of the sterol-containing membranes imply that a certain type of sterols such as **1**, **3**, and **5** promote the insertion of AmB into a POPC

membrane and the formation of AmB assemblies, some of which may act as ion channels.

In contrast, the sterol-dependent lifetime of the AmB complex in membrane (Supporting Information Figure S2) is not correlated very well with the sterol's effect on the AmB-induced K^+ influx among sterols bearing different side chains. In particular, Cho-type **5** possesses a significantly longer lifetime than Erg-type **2** but shows much weaker effect on the AmB activity than **2** (Figure 3). This inconsistency may be accounted for by formation of AmB dense aggregates in the presence of sterols **5**, **6**, and **7** with a Cho-type side chain as discussed above. The AmB aggregates in the membrane containing these sterols, which may not show prominent K^+ influx activity,[30] probably have a long lifetime.

CP-MAS Solid State NMR. In order to directly observe AmB-Erg and AmB-Cho interactions in the membrane, we measured solid state NMR spectra using hydrated POPC liposomes containing 4-^{13}C-Erg and 4-^{13}C-Cho, the former of which was newly synthesized as described in the Supporting Information. Figure 5 shows the ^{13}C CP-MAS NMR spectra of
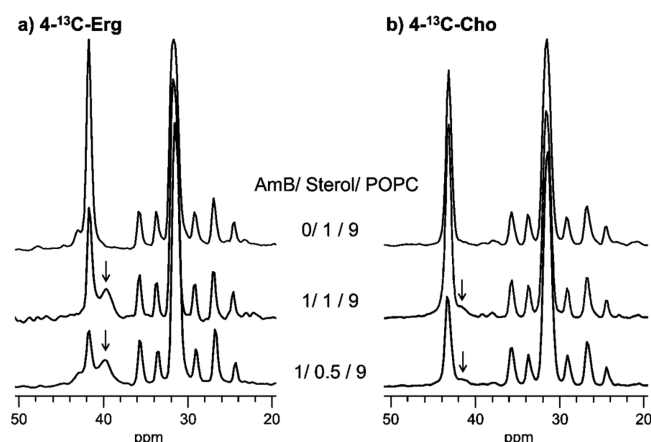

Figure 5. CP-MAS ^{13}C NMR spectra of 4-^{13}C-Erg (a) and 4-^{13}C-Cho (b) with the different concentrations of AmB in hydrated POPC membranes at 30 °C. The membrane preparation contained AmB/ 4-^{13}C-sterol/POPC at the molar ratios of 0:1:9 (top), 1:1:9 (middle), and 1:0.5:9 (bottom) in 10 mM HEPES/D$_2$O (50 wt %) at pH 7.0. Arrows indicated the 4-^{13}C signals of the sterols interacting with AmB.

the labeled sterols with the different concentrations of AmB. In the absence of AmB, the C4 signals of labeled Erg **1** and Cho **6** appear as sharp peaks at 42.3 and 43.4 ppm, respectively, which correspond to unbound sterols. In the case of the Erg-containing membrane, upon the addition of AmB, a broad peak appeared at 39.7 ppm (indicated by arrows in Figure 5), while the signal intensity at 42.3 ppm decreased. It is reported that a similar shifted signal was also observed for 26,27-^{13}C-Erg.[41] This signal shift was caused by the close contact between Erg and AmB, as described later, indicating the formation of stable AmB-Erg complexes. For the Cho-containing membrane, a broad signal appeared at 40.7 ppm by addition of AmB (indicated by arrows in Figure 5); however, the intensity of the new peak was very small, indicating that Cho interacted with AmB weakly in the membrane. These differences in NMR spectra clearly demonstrate that the affinity of AmB to Erg is much higher than that of AmB to Cho.

REDOR Experiments. To further confirm the differences in the intermolecular interactions between AmB/Erg and AmB/ Cho, we attempted to estimate their intermolecular distance by

$^{13}C\{^{19}F\}$REDOR, which was often used to obtain the structural information on AmB–AmB and AmB–lipid complexes in membranes.[30,31] In this experiment, we focused on the intermolecular interaction between the AmB macrolide ring and the steroid core using a combination of 14-F-AmB (Figure 1) and 4-^{13}C-sterol for $^{13}C\{^{19}F\}$REDOR. To exclude the motional averaging of dipolar coupling due to lateral diffusion of sterol, the REDOR spectra were recorded at −30 °C. Figure 6 shows the aliphatic region of nonirradiated (black trace for

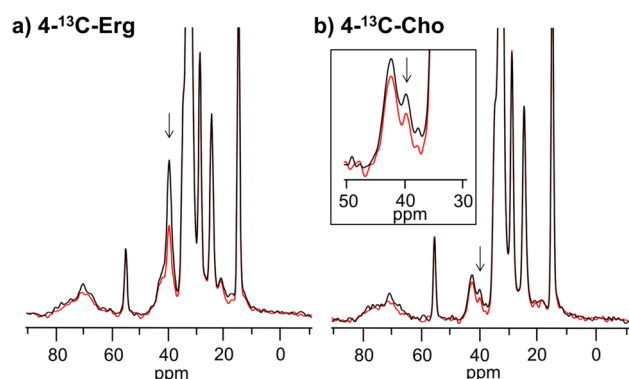**Figure 6.** $^{13}C\{^{19}F\}$REDOR spectra for 14-F-AmB/4-^{13}C-Erg/POPC (a) and 14-F-AmB/4-^{13}C-Cho/POPC (b) at the ratio of 1:1:9 in 10 mM HEPES/D$_2$O (50 wt %) at pH 7.0. Nonirradiated (full-echo) (S_0) spectra and ^{19}F-irradiated spectra (S) were expressed as black and red traces, respectively. Data were obtained after a ^{19}F dephasing period of 32 rotor cycles (6.4 ms) at −30 °C with (a) 25 208 and (b) 100 865 scans. The arrows depict the C4 signals of bound sterols. Expanded spectra around the C4 signal of Cho are inset.

S_0) and ^{19}F-irradiated (red line for S) spectra, where 14-F AmB/4-^{13}C-Erg (a) and 14-F-AmB/4-^{13}C-Cho (b) were mixed at a 1:1 ratio in hydrated POPC bilayers. Compared to the CP-MAS spectra measured at 30 °C (Figure 5), the intensity of the signal from unbound sterols was significantly decreased, whereas the peaks assigned to AmB-bound sterol (indicated by the arrows in Figure 6) were greatly enhanced. These changes in peak intensity were caused by a loss of mobility of the unbound sterols, as generally observed for bulk lipids in the gel phase.[55,56] The magnitudes of the REDOR dephasing effects were approximately 40% and 30% for 4-^{13}C-Erg and 4-^{13}C-Cho, respectively. This result demonstrated that the distance between the AmB macrolide and the A-ring of Erg was significantly shorter than that the corresponding distance to

that of Cho; their accurate distances could not be determined from the REDOR data mainly due to the overlapping of the signal of free 4-^{13}C-Cho with the weak signal of bound Cho. These solid state NMR experiments suggest that small differences in the structure of Erg and Cho greatly influence the stability of the AmB–sterol complex and the nature of the AmB–sterol interaction, and also imply that Erg forms more stable complexes with AmB. The further REDOR experiments for determining the interatomic distance between Erg and AmB are now underway and will be published in due course.

Conformation Analysis. In order to examine the interaction between AmB and alicyclic sterol structures in more detail, we investigated the conformational preference of sterol analogues by DFT calculations (Figure 7). Notably, the A-ring of Δ5,7,9-triene alicyclic compounds **4** and **8** becomes grossly out-of-plane as compared with that of the other sterols. This uneven tetracyclic face probably inhibits close contact between the sterol core and the macrolide of AmB (Figure 8B),
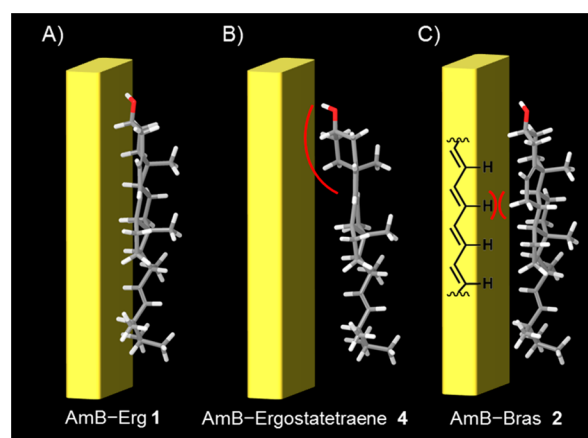

Figure 8. Putative illustration of schemes accounting for the high affinity of Erg **1** and the low affinity of **4** and **2** with AmB (yellow box). (A) Erg can closely interact with the macrolide of AmB due to its flat alicyclic structure. (B) Protruded A-ring of ergostatetraene hinders face-to-face contact with AmB. (C) Steric hindrance between the C7 axial hydrogen (H7$_{ax}$) of the sterol and the heptaene hydrogen of AmB inhibit face-to-face contact.

consequently reducing their VDW interaction. Other sterols showed similar alicyclic conformations with suitable planarity for interacting with AmB. A small distortion of the B-ring was observed for Δ5 sterols **2** and **6** as described by Langlet et al.[33]
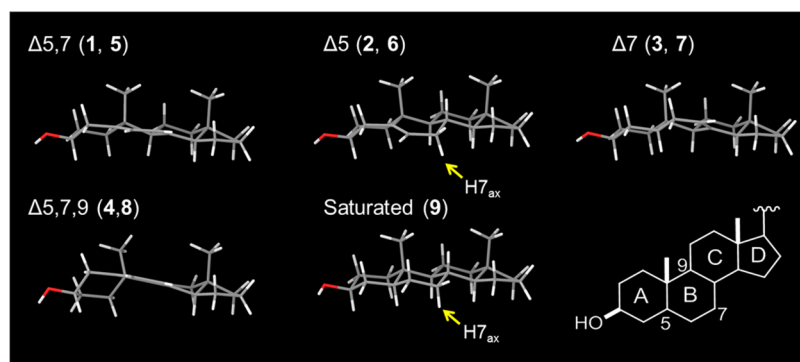

Figure 7. Preferable conformations of steroid cores for analogues **1−9** generated by DFT calculations. The side chains are omitted for clarity. The yellow arrows indicate the axial hydrogen atom at C7. The entire structures of sterol analogues were shown in Supporting Information Figure S5.

However, these Δ5 sterols and the fully saturated sterol **9** showed the significantly weaker activity than the activity of Δ5,7 and Δ7 sterols (Figures 2 and 3).

These results agree with the suggestion by Clejan and Bittman that the Δ7-double bond is essential for the sterol/AmB interaction.[25] The major structural alteration between **2** and **3**, which showed the significantly different K+-flux activities (Figure 3B), occurs in the C6−C7 portion, more specifically, the presence or absence of the axial hydrogen atom at C7 (H7ax) (Figure 7, yellow arrows). This C7 hydrogen may cause steric hindrance with the AmB macrolide by inhibiting VDW interaction. This effect of H7ax is also supported by the similar affinities of 7-keto-cholesterol and Erg for AmB, as described by Charbonneau et al.[24] The results of the solid state NMR experiments further reinforce this notion by demonstrating that the A-ring of Erg comes closer to the macrolide of AmB than Cho does. Both of the protrusion of ring A and the axial hydrogen atom at C7 are directed to the opposite side of the angular methyl group (α-face), indicating that the α-face of the sterol tetracyclic core interacts with AmB and consequently strengthens their VDW contact. Because the hydrophobic region of the drug interacts with sterol,[37,57] it is likely that the steric repulsion between the axial proton at C7 of the sterol and olefinic protons of AmB inhibits the face-to-face contact between these molecules (Figure 8C). Similar sterol recognition has been reported for other polyene macrolides such as natamycin, which requires the Δ7-double bond to interact with sterol, whereas the Δ5-double bond is not essential.[58] Therefore, it is reasonable to assume that such face-to-face contact is a common mechanism for sterol recognition of polyene macrolides that show selective binding with Erg.

In addition to these hydrophobic interactions, hydrogen bonding between AmB and sterols also has been a subject of research.[35,37,59−62] Previous experiments[59,60] and calculations[61,62] implied that the 2′-OH group of the mycosamine moiety plays an important role in intermolecular hydrogen bonding between sterols and AmB. Alternatively, a very recent report by Wilcock et al. revealed that the C2′OH is required for binding Cho but not Erg,[63] demonstrating that much remains to be understood about the AmB−sterol binding interactions. Since the effect of unsaturation in the B-ring on the AmB−sterol interactions, including hydrogen bonds, is a crucial issue for elucidating the atomistic mechanism of the sterol selectivity by AmB, further investigation on structure−activity relationship coupled with structural information on their complexes is essential.

In this study, we examined the ion-flux activity of AmB using sterol analogues with diverse alicyclic structures, and our results showed that the position of the double bond on the sterol core significantly affected the activity of AmB. Additionally, the UV spectra and SPR measurements of membrane-bound AmB revealed that the double bond profile of sterols greatly influences the stabilization of the AmB−sterol complex. As described above, it is generally considered that the conjugated double bonds of Erg facilitate VDW surface contact[24,33,37,64] and/or π−π electronic interactions[35,39] with AmB, and consequently AmB shows higher affinity to Erg than Cho. Our results, however, revealed that Δ5,7,9-sterols (**4**, **8**) had significantly weaker efficacy than those of other less unsaturated sterols, indicating that π−π electronic interaction may not be the primary factor for the drug's sterol-selectivity. The solid state NMR and conformational analysis suggested that the axial hydrogen atom at C7 reduces the binding affinity of the sterol

with AmB by inhibiting their close face-to-face contact. These results also provide new insight into the manner of AmB−sterol interaction: the flat α-face of the sterol alicycle interacts with the macrolide of AmB. In addition, the alicyclic steroid backbone and the sterol side chain contribute to their affinity for AmB in a relatively independent manner. These findings may help us develop a more efficacious and less toxic antifungal drug.

■ ASSOCIATED CONTENT

⑤ Supporting Information

The sensor grams of SPR experiments, the UV spectrum for POPC in sucrose buffer, synthesis of 4-^{13}C-Erg, and the entire structure of the sterol analogues generated by DFT calculations. This material is available free of charge via the Internet at http://pubs.acs.org.

■ AUTHOR INFORMATION

Corresponding Authors

*E-mail matsmori@chem.kyushu-univ.jp. Phone (+81)-9-2642-2582.
*E-mail murata@chem.sci.osaka-u.ac.jp. Phone (+81)-6-6850-5774. Fax (+81)-6-6850-5774.

Present Address

Tohru Oishi and Nobuaki Matsumo, Department of Chemistry, Graduate School of Sciences, Kyushu University, 6−10−1 Hakozaki, Higashi-ku, Fukuoka, 812−8581, Japan

Notes

The authors declare no competing financial interest.

■ ABBREVIATIONS

AmB, amphotericin B; BCECF, 2′,7′-bis(carboxyethyl)-4(5)-carboxyfluorescein; Bras, brassicasterol; Cho, cholesterol; CP-MAS, cross-polarization magic angle spinning; 7-DHC, 7-dehydrocholesterol; Erg, ergosterol; FCCP, carbonyl cyanide-*p*-trifluoro-methoxy-phenyl hydrazine; POPC, 1-palmitoyl-2-oleoyl-*sn*-glycero-3-phosphocholine; REDOR, rotational echo double resonance; SPR, surface plasmon resonance

■ REFERENCES

(1) Bolard, J. (1986) How do the polyene macrolide antibiotics affect the cellular membrane properties? *Biochim. Biophys. Acta* 864, 257−304.

(2) Sugiyama, R., Nishimura, S., Matsumori, N., Tsunematsu, Y., Hattori, A., and Kakeya, H. (2014) Structure and biological activity of 8-deoxyheronamide C from a marine-derived Streptomyces sp.: heronamides target saturated hydrocarbon chains in lipid membranes. *J. Am. Chem. Soc.* 136, 5209−5212.

(3) Espiritu, R. A., Matsumori, N., Tsuda, M., and Murata, M. (2014) Direct and stereospecific interaction of amphidinol 3 with sterol in lipid bilayers. *Biochemistry* 53, 3287−3293.

(4) Houdai, T., Matsuoka, S., Matsumori, N., and Murata, M. (2004) Membrane-permeabilizing activities of amphidinol 3, polyene-poly-hydroxy antifungal from a marine dinoflagellate. *Biochim. Biophys. Acta* 1667, 91−100.

(5) Houdai, T., Matsuoka, S., Morsy, N., Matsumori, N., Satake, M., and Murata, M. (2005) Hairpin conformation of amphidinols possibly accounting for potent membrane permeabilizing activities. *Tetrahedron* 61, 2795−2802.

(6) Morsy, N., Houdai, T., Matsuoka, S., Matsumori, N., Adachi, S., Oishi, T., Murata, M., Iwashita, T., and Fujita, T. (2006) Structures of new amphidinols with truncated polyhydroxyl chain and their membrane-permeabilizing activities. *Bioorg. Med. Chem.* 14, 6548−6554.

(7) Nishimura, S., Arita, Y., Honda, M., Iwamoto, K., Matsuyama, A., Shirai, A., Kawasaki, H., Kakeya, H., Kobayashi, T., Matsunaga, S., and Yoshida, M. (2010) Marine antifungal theonellamides target 3β-hydroxysterol to activate Rho1 signaling. *Nat. Chem. Biol.* 6, 519−526.

(8) Espiritu, R. A., Matsumori, N., Murata, M., Nishimura, S., Kakeya, H., Matsunaga, S., and Yoshida, M. (2013) Interaction between the marine sponge cyclic peptide theonellamide A and sterols in lipid bilayers as viewed by surface plasmon resonance and solid-state ^{2}H nuclear magnetic resonance. *Biochemistry* 52, 2410−2418.

(9) Matsumori, N., Tahara, K., Yamamoto, H., Morooka, A., Doi, M., Oishi, T., and Murata, M. (2009) Direct interaction between amphotericin B and ergosterol in lipid bilayers as revealed by ^{2}H NMR spectroscopy. *J. Am. Chem. Soc.* 131, 11855−11860.

(10) Ostrosky-Zeichner, L., Marr, K. a, Rex, J. H., and Cohen, S. H. (2003) Amphotericin B: time for a new "gold standard. *Clin. Infect. Dis.* 37, 415−425.

(11) Lemke, A., Kiderlen, A. F., and Kayser, O. (2005) Amphotericin B. *Appl. Microbiol. Biotechnol.* 68, 151−162.

(12) Martin, C. A. (2005) Invasive fungal infections in the critically ill patient. *J. Pharm. Pract.* 18, 9−17.

(13) Duarte, J. M., Betts, R., Rotstein, C., Colombo, A. L., Moya, L. T., Smietana, J., Lupinacci, R., Sable, C., Kartsonis, N., and Perfect, J. (2002) Comparison of caspofungin and amphotericin B for invasive candidiasis. *N. Engl. J. Med.* 347, 2020−2029.

(14) De Kruijff, B., and Demel, R. A. (1974) Polyene antibiotic-sterol interactions in membranes of acholeplasma laidlawii cells and lecithin liposomes. III. molecular structure of the polyene antibiotic-cholesterol complexes. *Biochim. Biophys. Acta* 339, 57−70.

(15) Kamiński, D. M. (2014) Recent progress in the study of the interactions of amphotericin B with cholesterol and ergosterol in lipid environments. *Eur. Biophys. J.* 43, 453−467.

(16) Barwicz, J., Gruda, I., and Tancre, P. (2000) A kinetic study of the oxidation effects of amphotericin B on human low-density lipoproteins. *FEBS Lett.* 465, 83−86.

(17) Sangalli-Leite, F., Scorzoni, L., Mesa-Arango, A. C., Casas, C., Herrero, E., Gianinni, M. J. S. M., Rodríguez-Tudela, J. L., Cuenca-Estrella, M., and Zaragoza, O. (2011) Amphotericin B mediates killing in Cryptococcus neoformans through the induction of a strong oxidative burst. *Microbes Infect.* 13, 457−467.

(18) Hartsel, S., and Bolard, J. (1996) Amphotericin B: new life for an old drug. *Trends Pharmacol. Sci.* 17, 445−449.

(19) Takano, T., Konoki, K., Matsumori, N., and Murata, M. (2009) Amphotericin B-induced ion flux is markedly attenuated in phosphatidylglycerol membrane as evidenced by a newly devised fluorometric method. *Bioorg. Med. Chem.* 17, 6301−6304.

(20) Anderson, T. M., Clay, M. C., Cioffi, A. G., Diaz, K. a, Hisao, G. S., Tuttle, M. D., Nieuwkoop, A. J., Comellas, G., Maryum, N., Wang, S., Uno, B. E., Wildeman, E. L., Gonen, T., Rienstra, C. M., and Burke, M. D. (2014) Amphotericin forms an extramembranous and fungicidal sterol sponge. *Nat. Chem. Biol.* 10, 400−406.

(21) Gray, K. C., Palacios, D. S., Dailey, I., Endo, M. M., Uno, B. E., Wilcock, B. C., and Burke, M. D. (2012) Amphotericin primarily kills yeast by simply binding ergosterol. *Proc. Natl. Acad. Sci. U. S. A.* 109, 2234−2239.

(22) Baginski, M., Czub, J., and Sternal, K. (2006) Interaction of amphotericin B and its selected derivatives with membranes: molecular modeling studies. *Chem. Rec.* 6, 320−332.

(23) Vertut-Croquin, A., Bolard, J., Chabbert, M., and Gary-Bobo, C. (1983) Differences in the interaction of the polyene antibiotic amphotericin B with cholesterol-or ergosterol-containing phospholipid vesicles. A circular dichroism and permeability study. *Biochemistry* 22, 2939−2944.

(24) Charbonneau, C., Fournier, I., Dufresne, S., Barwicz, J., and Tancrède, P. (2001) The interactions of amphotericin B with various sterols in relation to its possible use in anticancer therapy. *Biophys. Chem.* 91, 125−133.

(25) Clejan, S., and Bittman, R. (1985) Rates of amphotericin B and filipin association with Sterols. *J. Biol. Chem.* 260, 2884−2889.

(26) Chen, W. C., and Bittman, R. (1977) Kinetics of association of amphotericin B with vesicles. *Biochemistry* 16, 4145−4149.

(27) Herve, M., Debouzy, J., Borowski, E., Cybulska, B., and Gary-bobo, C. M. (1989) The role of the carboxyl and amino groups of polyene macrolides in their interactions with sterols and their selective toxicity. A ^{31}P-NMR study. *Biochim. Biophys. Acta* 980, 261−272.

(28) Hsuchen, C. C., and Feingold, D. S. (1973) Selective membrane toxicity of the polyene antibiotics: studies on lecithin membrane models (liposomes). *Antimicrob. Agents Chemother.* 4, 309−315.

(29) Matsuoka, S., and Murata, M. (2002) Cholesterol markedly reduces ion permeability induced by membrane-bound amphotericin B. *Biochim. Biophys. Acta* 1564, 429−434.

(30) Umegawa, Y., Matsumori, N., Oishi, T., and Murata, M. (2008) Ergosterol increases the intermolecular distance of amphotericin B in the membrane-bound assembly as evidenced by solid-state NMR. *Biochemistry* 47, 13463−13469.

(31) Umegawa, Y., Nakagawa, Y., Tahara, K., Tsuchikawa, H., Matsumori, N., Oishi, T., and Murata, M. (2012) Head-to-tail interaction between amphotericin B and ergosterol occurs in hydrated phospholipid membrane. *Biochemistry* 51, 83−89.

(32) Matsuoka, S., Ikeuchi, H., Matsumori, N., and Murata, M. (2005) Dominant formation of a single-length channel by amphotericin B in dimyristoylphosphatidylcholine membrane evidenced by ^{13}C-^{31}P rotational echo double resonance. *Biochemistry* 44, 704−710.

(33) Langlet, J., Bergès, J., Caillet, J., and Demaret, J. (1994) Theoretical study of the complexation of amphotericin B with sterols. *Biochim. Biophys. Acta* 1191, 79−93.

(34) Baginski, M., Resat, H., and Borowski, E. (2002) Comparative molecular dynamics simulations of amphotericin B-cholesterol/ergosterol membrane channels. *Biochim. Biophys. Acta* 1567, 63−78.

(35) Baran, M., Borowski, E., and Mazerski, J. (2009) Molecular modeling of amphotericin B-ergosterol primary complex in water II. *Biophys. Chem.* 141, 162−168.

(36) Neumann, A., Czub, J., and Baginski, M. (2009) On the possibility of the amphotericin B-sterol complex formation in cholesterol- and ergosterol-containing lipid bilayers: a molecular dynamics study. *J. Phys. Chem. B* 113, 15875−15885.

(37) Neumann, A., Baginski, M., and Czub, J. (2010) How do sterols determine the antifungal activity of amphotericin B? Free energy of binding between the drug and its membrane targets. *J. Am. Chem. Soc.* 132, 18266−18272.

(38) Nakagawa, Y., Umegawa, Y., Takano, T., Tsuchikawa, H., Matsumori, N., and Murata, M. (2014) Effect of sterol side chain on ion channel formation by amphotericin B in lipid bilayers. *Biochemistry* 53, 3088−3094.

(39) Baginski, M., and Borowski, E. (1997) Distribution of electrostatic potential around amphotericin B and its membrane targets. *J. Mol. Struct. THEOCHEM* 389, 139−146.

(40) Baginski, M., Bruni, P., and Borowski, E. (1994) Comparative analysis of the distribution of the molecular electrostatic potential for cholesterol and ergosterol. *J. Mol. Struct. THEOCHEM* 311, 285−296.

(41) Giroux, S., and Corey, E. J. (2008) An efficient, stereocontrolled synthesis of the 25-(R)-diastereomer of dafachronic acid A from beta-ergosterol. *Org. Lett.* 10, 801−802.

(42) Delseth, C., Kashman, Y., and Djerassi, C. (1979) Ergosta-5,7,9(11),22-tetraen-3β-ol and its 24ξ-ethyl Homolog, two new marine sterols from the red sea sponge biemna fortis. *Helv. Chim. Acta 62*, 2037−2045.

(43) Ohvo-Rekilä, H., Akerlund, B., and Slotte, J. P. (2000) Cyclodextrin-catalyzed extraction of fluorescent sterols from monolayer membranes and small unilamellar vesicles. *Chem. Phys. Lipids 105*, 167−178.

(44) Pelc, B., and Kodicek, E. (1972) Synthesis of [4-14C] Ergosterol and [4-14C] Ergocalcifero. *J. Chem. Soc., Perkin Trans. 1*, 2980−2981.

(45) Bennett, A. E., Rienstra, C. M., Auger, M., Lakshmi, K. V., and Griffin, R. G. (1995) Heteronuclear decoupling in rotating solids. *J. Chem. Phys. 103*, 6951−6958.

(46) Gullion, T., Baker, D., and Conradi, M. (1990) New, compensated carr-purcell sequences. *J. Magn. Reson. 89*, 479−484.

(47) Kolossváry, I., and Guida, W. (1999) Low-mode conformational search elucidated: Application to $C_{39}H_{80}$ and flexible docking of 9-deazaguanine inhibitors into PNP. *J. Comput. Chem. 20*, 1671−1684.

(48) Kaminski, G., and Friesner, R. (2001) Evaluation and reparametrization of the OPLS-AA force field for proteins via comparison with accurate quantum chemical calculations on peptides. *J. Phys. Chem. B 2*, 6474−6487.

(49) Polak, E. (1971) *Computational methods in optimization*, Academic Press, New York.

(50) Ponder, J. W., and Richards, F. M. (1987) An efficient newton-like method for molecular mechanics energy minimization of large molecules. *J. Comput. Chem. 8*, 1016−1024.

(51) Parr, R., and Yang, W. (1994) *Density-functional theory of atoms and molecules*, pp 47−86, Oxford University Press, New York.

(52) Becke, A. D. (1988) Density-fnnctional exchange-energy approximation with correct asymptotic behavior. *Phys. Rev. A 38*, 3098−3100.

(53) Fujii, G., Chang, J. E., Coley, T., and Steere, B. (1997) The formation of amphotericin B ion channels in lipid bilayers. *Biochemistry 36*, 4959−4968.

(54) Gagoś, M., Koper, R., and Gruszecki, W. I. (2001) Spectrophotometric analysis of organisation of dipalmitoylphosphatidylcholine bilayers containing the polyene antibiotic amphotericin B. *Biochim. Biophys. Acta 1511*, 90−98.

(55) Bruzik, K. S., Salamonczyk, G. M., and Sobon, B. (1990) 13C CP-MAS study of the gel phases of 1,2-dipalmitoylphosphatidylcholine. *Biochim. Biophys. Acta 1023*, 143−146.

(56) Bruzik, K. S., and Harwood, J. S. (1997) Conformational study of phospholipids in crystalline state and hydrated bilayers by 13C and 31P CP-MAS NMR. *J. Am. Chem. Soc. 119*, 6629−6637.

(57) Baran, M., and Mazerski, J. (2002) Molecular modelling of amphotericin B−ergosterol primary complex in water. *Biophys. Chem. 95*, 125−133.

(58) Te Welscher, Y. M., ten Napel, H. H., Balagué, M. M., Souza, C. M., Riezman, H., de Kruijff, B., and Breukink, E. (2008) Natamycin blocks fungal growth by binding specifically to ergosterol without permeabilizing the membrane. *J. Biol. Chem. 283*, 6393−6401.

(59) Matsumori, N., Sawada, Y., and Murata, M. (2005) Mycosamine orientation of amphotericin B controlling interaction with ergosterol: sterol-dependent activity of conformation-restricted derivatives with an amino-carbonyl bridge. *J. Am. Chem. Soc. 127*, 10667−10675.

(60) Croatt, M., and Carreira, E. (2011) Probing the role of the mycosamine C2′-OH on the activity of amphotericin B. *Org. Lett. 13*, 1390−1393.

(61) Silberstein, A. (1998) Conformational analysis of amphotericin B — Cholesterol channel complex. *J. Membr. Biol. 126*, 117−126.

(62) Czub, J., Neumann, A., Borowski, E., and Baginski, M. (2009) Influence of a lipid bilayer on the conformational behavior of amphotericin B derivatives - A molecular dynamics study. *Biophys. Chem. 141*, 105−116.

(63) Wilcock, B. C., Endo, M. M., Uno, B. E., and Burke, M. D. (2013) C2′-OH of amphotericin B plays an important role in binding the primary sterol of human cells but not yeast cells. *J. Am. Chem. Soc. 135*, 8488−8491.

(64) Baginski, M., Tempczyk, A., and Browski, E. (1989) Comparative conformational analysis of cholesterol and ergosterol by molecular mechanics. *Eur. Biophys. J. 17*, 159−166.